Clay Minerals (2003) **38**, 259–278

Novel nuclear magnetic resonance techniques for the study of quadrupolar nuclei in clays and other layered materials

J. ROCHA[1,*], C. M. MORAIS[1,2] AND C. FERNANDEZ[2]

[1] *Department of Chemistry, CICECO, University of Aveiro, 3810-193 Aveiro, Portugal, and* [2] *Laboratoire Catalyse et Spectrochimie (CNRS UMR 6506), ENSICAEN, 14050 Caen, France*

(*Received 8 July 2003; revised 28 July 2003*)

ABSTRACT: The main developments taking place in Nuclear Magnetic Resonance Spectroscopy (NMR) of quadrupolar (spin $I > 1/2$) nuclei with half integer spins in solids, particularly clays and other layered materials, have been reviewed. The advent of Multiple-Quantum (MQ) Magic-Angle Spinning (MAS) NMR spectroscopy has been a step-change development to the studies of quadrupolar nuclei in solids. It is now possible to record high-resolution spectra of important nuclei, such as ^{11}B, ^{17}O, ^{23}Na, ^{27}Al and ^{69,71}Ga, in synthetic and natural clays. Since its introduction in 1995 MQMAS NMR has evolved considerably and, at present, a range of very useful related techniques are available and have been reviewed, as has the current situation with regard to applications to clays and other layered materials.

KEYWORDS: nuclear magnetic resonance spectroscopy, quadrupolar nuclei, clay, radio-frequency radiation, STMAS, MQMAS.

Nuclear magnetic resonance spectroscopy is a tool which is used increasingly to study solids, including a variety of silicates and layered materials such as clays. To a certain extent, NMR is now a routine technique available to solid-state chemists and mineralogists. However, an approach which is too simplistic can give misleading results, particularly when dealing with quadrupolar nuclei (those with spin $I > 1/2$). Moreover, in the last decade or so many novel pulse sequences became available, yielding valuable information on the structure and molecular dynamics in solids. It is, thus, time for a review to set out the different approaches and, through examples, to explain what has been achieved to date. Here, we shall concentrate on the main developments which are taking place in the field of quadrupolar nuclei with half integer spins.

* E-mail: rocha@dq.ua.pt
DOI: 10.1180/0009855033830094

Several NMR-active nuclei are available to study clays and related materials. Some of these are $I = 1/2$ nuclei with a low natural abundance (e.g. ^{29}Si) or they may be ~100% abundant (e.g. ^{1}H). Over 70% of all NMR active nuclei are quadrupolar, with integer (e.g. ^{2}H, $I = 1$) or half-integer (e.g. ^{27}Al, $I = 5/2$) spin. Normally, NMR spectra cannot be recorded in the same manner for solids as for liquids. This is because in the solid state, one has to consider a number of anisotropic interactions, which can be overlooked for solutions as the random molecular tumbling averages the NMR interactions to isotropic values. These interactions broaden the NMR spectral lines of solids considerably. For $I = 1/2$ nuclei a number of methods are well established for eliminating or reducing significantly the effects of the broadening interactions, affording high-resolution solid-state NMR spectra. In contrast, narrowing the spectral lines of half-integer quadrupolar nuclei is a particularly challenging task and has attracted the efforts of

NMR spectroscopists in the last 15 years or so. The introduction in 1995 of Multiple-Quantum (MQ) Magic-Angle Spinning (MAS) NMR spectroscopy prompted a revolution in this field. It is now possible to record high-resolution NMR spectra of half-integer quadrupolar nuclei in solids. MQMAS NMR has evolved and many new techniques have been proposed for improving its efficiency and allowing the extraction of information of chemical interest.

In this review we shall introduce some basic concepts about solid-state NMR of half-integer quadrupolar nuclei and discuss the most useful and promising methods currently available to study them. These include older methods, such as Double Rotation (DOR) and Dynamic Angle Spinning (DAS), and novel techniques including MQMAS, Quadrupolar Phase Adjusted Spinning Sidebands QPASS, Satellite Transition (ST) MAS and Inverse-STMAS NMR. We also discuss several techniques based on dipolar interactions between quadrupolar and spin-1/2 nuclei, such as Cross-Polarization (CP) MQMAS, MQ Heteronuclear Correlation Spectroscopy (HETCOR), MQ REDOR (Rotational Echo Double Resonance), TRAPDOR (Transfer of populations in Double Resonance) and REAPDOR (Rotational Echo Adiabatic Passage Double Resonance). This review also covers the available literature on application of these techniques to clays and other layered materials.

QUADRUPOLAR NUCLEI: BASIC IDEAS

Solid-state NMR spectra of quadrupolar nuclei (spin $I > 1/2$) are broadened by the electric quadrupole interaction. These nuclei have a non-spherically symmetrical distribution of nuclear charge and possess an electric quadrupole moment, which interacts strongly with any electric field gradient (created by the surrounding electron cloud) at the site of the nucleus. The size of the quadrupolar interaction can be described by the quadrupolar frequency ν_Q, which is proportional to the quadrupolar moment Q of the nucleus and to the electric field gradient (EFG). The quadrupolar frequency is defined as $\nu_Q = C_Q/[2I(2I+1)]$, where C_Q is the quadrupolar coupling constant defined in terms of one of the principal values of the EFG tensor ($V_{zz} = eq$) as $C_Q = e^2qQ/h$. Depending on the size of Q and on the local electronic environment, ν_Q can be several MHz.

In most cases, the quadrupolar interaction is smaller than the Zeeman splitting of energy levels and we can calculate its influence by perturbation theory. A spin I nucleus has $(2I+1)$ equidistant energy levels due to its interaction with the external static magnetic field B_0 (Zeeman interaction). These energy levels are usually labelled with their magnetic quantum number $m = -I, -I+1,...+I$ and the energy difference between two consecutive levels is given in frequency units by the Larmor frequency ν_0. For the quadrupole interaction, energy corrections up to second order are generally needed.

To first order, the quadrupole interaction has no effect on the symmetric transitions, namely on the central transition $m = 1/2 \rightleftharpoons m' = -1/2$ or on the multi-quantum transitions ($m = 3/2 \rightleftharpoons m' = -3/2$, $m = 5/2 \rightleftharpoons m' = -5/2$...). Only the satellite transitions ($m = \pm1/2 \rightleftharpoons m' = \pm3/2$, $m = \pm3/2 \rightleftharpoons m' = \pm5/2$, ...) are affected and for these the first-order quadrupolar effect is of the order of ν_Q (MHz range). Thus, in a powdered sample, the NMR spectrum spreads over a frequency range which, for many nuclei, exceeds the bandwidth of the spectrometer.

The central, $m = 1/2 \rightleftharpoons m' = -1/2$, transition is affected by the quadrupolar interaction to second order. Because the contribution of the second-order quadrupole terms is typically 10^2 to 10^3 (kHz range) smaller than ν_Q, the central transition yields a narrower and more intense line in the NMR spectrum, which has been the subject of most of the studies on half-integer quadrupolar nuclei. Figure 1 shows the effect of the first and second-order quadrupolar interactions for a spin-3/2 nucleus.

The second-order energy correction caused by the quadrupolar interaction contains an isotropic term. This is very important as it means that the NMR isotropic shifts of quadrupolar nuclei have a contribution from the quadrupole coupling in addition to the usual chemical shift. As a result, the centre of gravity of the NMR lines is shifted by an amount which depends on the quadrupole coupling parameters (quadrupole coupling constant and asymmetry parameter) of the nucleus under study and the magnetic field. Some caution is therefore needed in the interpretation of NMR spectra of quadrupolar nuclei. The true isotropic shift can only be calculated when the quadrupole coupling parameters are known. Furthermore, the second-order energy correction depends inversely on the Larmor frequency and, hence, the importance of this term decreases with increasing field strength. The isotropic quadrupolar shift and the

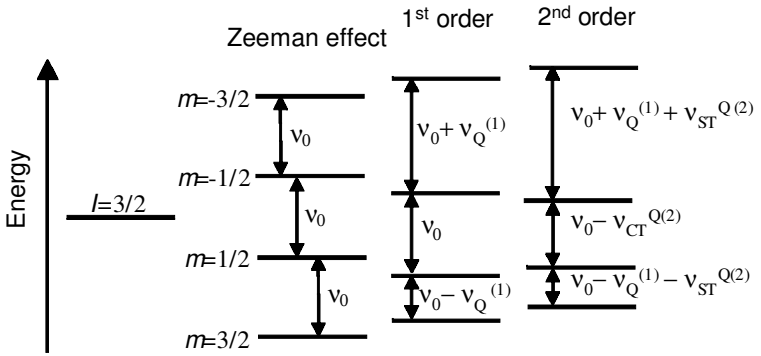

FIG. 1. Energy levels of a spin-3/2 quadrupolar nucleus in the presence of Zeeman interaction and first- and second-order quadrupole interactions.

width of the powder patterns are inversely proportional to the external magnetic field. In general, therefore, it is desirable to work at a magnetic field as high as possible because the NMR peaks are sharper at high fields and the spectra are simplified.

EFFECT OF RADIO FREQUENCY IRRADIATION ON QUADRUPOLAR NUCLEI

In general, the interaction of nuclei with the radio-frequency (r.f.) field is much stronger than any internal nuclear spin interaction and, therefore, the latter may be ignored during r.f. irradiation. However, the strength of the first-order quadrupolar interaction is often larger than the strength of the interaction of the nuclei with the r.f. field and it cannot be ignored during the pulse. Hence, for quadrupolar nuclei, during the r.f. pulse, one must include in the Hamiltonian the term corresponding to the first-order quadrupolar interaction, in addition to the Zeeman and r.f. terms (Samoson & Lippmaa, 1983; Fenzke *et al.*, 1984; Man *et al.*, 1988).

Figure 2 shows the signal intensity corresponding to the central transition of spin I = 3/2 and 5/2 nuclei as a function of the pulse-flip angle, the angle through which the magnetization has been tilted away from the equilibrium position (which is along the rotating frame z axis) by the r.f. pulse (Levitt, 2001), for different values of ν_Q/ν_1 (ν_1 is the r.f. field amplitude). These results were obtained by numerical calculations using the programme PULSAR (Amoureux *et al.*, 1995). Satellite transitions exhibit a similar behaviour but with different signal amplitudes and frequencies. A general picture of the behaviour of quadrupolar nuclei under r.f. irradiation may be obtained considering the following cases:

(1) $\nu_1 >> \nu_Q$, all transitions are effectively on resonance (non-selective excitation). Each transition has a sinusoidal evolution frequency ν_1, as a function of the flip angle.

(2) $\nu_Q >> \nu_1$ selective excitation of the on-resonance transition occurs. We assume no irradiation on the other transitions, so that only the on-resonance (m, m+1) transition needs to be considered, as if these were the only two spin levels present. It may be shown that the evolution of the on-resonance transition is sinusoidal, with frequency $[I(I+1)-m(m-1)]^{1/2}\nu_1$. In particular, for the central transition the pulse corresponding to the maximum signal intensity (selective or 'solid' $\pi/2$ pulse) is:

$$\left(\frac{\pi}{2}\right)_{\text{selective}} = \frac{1}{(I+1/2)}\left(\frac{\pi}{2}\right)_{\text{non-selective}} \qquad (1)$$

(3) $\nu_Q \approx \nu_1$, the excitation degree depends on ν_1, ν_Q and on the molecular orientation in the applied field. In a powdered sample, nuclei in equivalent sites but in different crystallites may experience different excitation. This results in distorted powder patterns and intensities that are not proportional to the number of nuclear spins corresponding to the different sites (non-quantitative spectra). The evolution of the system is not periodic and it is possible to excite multi-quantum coherences with a single pulse.

For quadrupolar nuclei, the dependence of the r.f. excitation on ν_Q is less important as the r.f. pulse length decreases. It has been shown that hard pulses

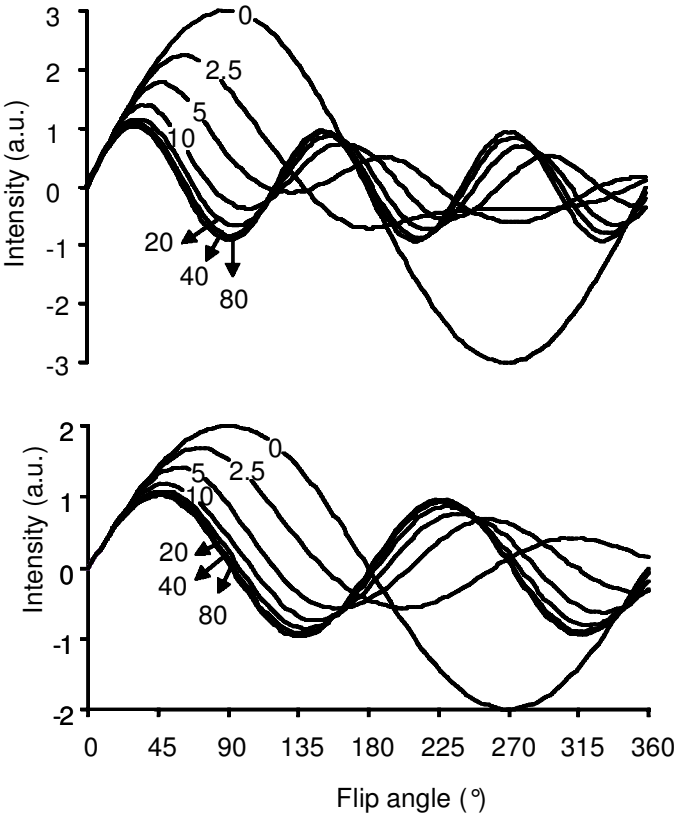

FIG. 2. Signal intensity of the central transition of $I = 3/2$ (bottom) and $I = 5/2$ (top) nuclei under r.f. irradiation as a function of the pulse flip angle, for different values of ν_Q/ν_1.

shorter than $\pi_{liquid}/[2(2I + 1)]$ provide homogeneous excitation of all quadrupolar nuclei in a powdered sample and, therefore, they are commonly used in NMR studies in order to obtain reliable relative intensities for different resonances.

HIGH-RESOLUTION NMR TECHNIQUES FOR STUDYING QUADRUPOLAR NUCLEI

Most solid-state NMR studies of quadrupolar nuclei in the past two decades use MAS for line narrowing. Although this technique can average out the first-order interactions (dipole-dipole coupling, chemical shift anisotropy) it is not able to remove the second-order quadrupolar interaction affecting, in particular, the central transition of quadrupolar nuclei. It can only sharpen the second-order quadrupole broadened lines by a factor of ~3, a performance that may be improved by spinning the samples at angles other than the magic angle, but can lead to complicated lineshapes.

Several techniques have been proposed for completely removing the anisotropic part of the second-order quadrupole interaction, providing isotropic spectra of half-integer quadrupole nuclei with unprecedented resolution. In Double Rotation (DOR) this is achieved by spinning the sample about two axes simultaneously, one inclined at the magic angle (54.74°) with respect to the external magnetic field, the other at either 30.6° or 70.1° to the first angle (Samoson *et al.*, 1988). In the two-dimensional Dynamic Angle Spinning (DAS) experiment the sample is spun sequentially about two different angles (37.4° and 79.2°) to the external magnetic field, for equal periods of time, with the magnetization stored by a *z*-filter pulse sequence during the angle-switching period (Chmelka *et al.*, 1989; Llor & Virlet, 1988). Much of the NMR signal may be lost in this

period when the sample relaxation is fast (as is often the case for quadrupole nuclei). This technique also has limitations in strongly dipolar-coupled systems (spin exchange due to dipolar interactions, which cannot be eliminated during the relatively long flipping time of the rotor axis, has to be sufficiently small). Both DOR and DAS require dedicated NMR probes and their implementation still poses technical problems.

Frydman & Harwood (1995) proposed a revolutionary new two-dimensional technique known as Multiple-Quantum (MQ) MAS NMR spectroscopy. In this experiment, the line narrowing of the central transition is achieved by the correlation of the phase evolutions of the symmetric MQ and single-quantum (1Q) transitions under MAS. The approach only requires a conventional MAS NMR probe and its practical implementation is relatively straightforward. The experiment has become quite widespread and has enabled new applications for a variety of nuclei possessing different spin quantum numbers and coupling environments such as ^{17}O, ^{23}Na, ^{27}Al, ^{87}Rb and ^{93}Nb.

The MQMAS experiment: principle and acquisition schemes

The simplest MQMAS NMR pulse sequence consists of two short and powerful r.f. pulses separated by a delay t_1, which is incremented in successive experiments (Fig. 3). The first pulse generates 1Q and MQ coherences (the presence of coherences ρ_+ and ρ_- indicates transverse spin magnetization, i.e. a net spin polarization perpendicular to the external B_0 field, see Levitt (2001) for a detailed discussion of populations and coherences in NMR). By carefully cycling the phase of this pulse it is possible to retain only symmetric MQ coherences with the quantum level pQ ($p/2 \rightleftharpoons -p/2$), which are free from first-order quadrupolar effects ($p = 2m$, thus $p = 3$ for the 3QMAS experiment, $p = 5$ for the 5QMAS experiment, and so on). After evolving during time t_1, the selected symmetric MQ coherence is selectively transferred into 1Q coherence, by the second pulse, and is observed during the acquisition time t_2. The flip angles of the first and second pulse must be optimized to yield the highest signal amplitude. The result depends on the nuclear spin I, Larmor frequency, chosen coherence order (pQ) and the ratio between the amplitude of the r.f. field and the quadrupolar frequency.

The key feature of the MQMAS experiment is that the anisotropic second-order quadrupolar broadening is averaged out when the ratio of times t_1 and t_2, spent on the quantum levels pQ and -1Q, fulfils the condition:

$$t_2 = p\frac{36I(I+1) - 17p^2 - 10}{36I(I+1) - 27}t_1 = R(I,p)t_1 \quad (2)$$

Isotropic echoes appear at time $t_2 = R(I,p)t_1$; for example, in an ^{27}Al triple-quantum ($I = 5/2$, $p = 3$) spectrum $R = 19/12$, while in a ^{23}Na triple-quantum ($I = 3/2$, $p = 3$) spectrum $R = -7/9$. After a double Fourier transformation in t_2 and t_1, the NMR resonances appear along the anisotropic axis A with direction $F_1 = R(I,p)F_2$, where F_2 and F_1 represent frequencies in the single- and multiple-quantum dimensions, respectively. The projection of the spectrum onto an axis perpendicular to axis A yields an isotropic, highly resolved, spectrum.

The sign of the ratio $R(I,p)$ is very important because it determines the relative sign of 3Q and 1Q coherences necessary to refocus the second-order broadening and form an isotropic echo at positive t_2 values. For spin $I = 3/2$ nuclei, this corresponds to the correlation of $p = -3$ and $p = -1$ coherences (solid line in Fig. 3) and for spins I

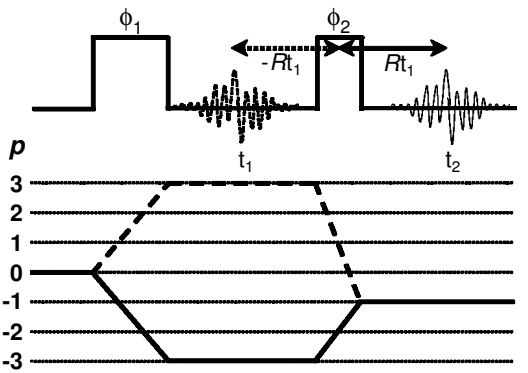

FIG. 3. Schematic diagram of the two-pulse 3QMAS NMR experiment (upper) and coherence transfer pathways (lower). This diagram represents the history of coherence orders p leading to the desired NMR signals in a particular experiment. All pathways start with order 0 (corresponding to spin populations) and terminate with order -1 (corresponding to observable (-1) quantum coherences detected; for details see Levitt, 2001). Isotropic echoes form at time $t_2 = R(I,p)t_1$. ϕ_1 and ϕ_2 are the phases of the first and second pulses, respectively.

= 5/2, 7/2, 9/2 to the correlation of $p = 3$ and $p = -1$ coherences (dashed line in Fig. 3). It is also useful to consider here the antiecho pathway, for which the anisotropic broadening is refocused at negative t_2 values.

If the phase cycling used only selects one coherence transfer pathway, a two-dimensional spectrum with (undesirable) 'phase-twist' lineshapes is observed (see Levitt, 2001, for details). However, the experiment can be easily modified to ensure that pure absorption (pure phase) lineshapes are obtained. The most commonly used modified acquisition schemes that allow pure-phase MQMAS spectra to be obtained include amplitude-modulated experiments with hypercomplex acquisition or phase-modulated experiments with delayed acquisition, such as shifted echo or antiecho and split-t_1 methods.

Amplitude-modulated experiments: (a) two-pulse experiments. In this type of experiment, the echo and antiecho are linearly combined with the same amplitude yielding an amplitude-modulated signal in t_1. Pure-absorption lineshapes are obtained in the frequency domain spectrum after a two-dimensional Fourier transform. The disadvantage of this method is that it is not possible to discriminate the sign of the MQ coherences evolving in t_1. Sign discrimination can be restored using the States (or the TPPI) method, which involves performing consecutively two experiments with a $90°/p$ phase shift of the first pulse, where p is the order of the coherence evolving during t_1. An important shortcoming of two-pulse methods is the difficulty of balancing the echo and antiecho amplitudes, in order to obtain undistorted two-dimensional lineshapes, especially for $I > 3/2$ nuclei. The two coherence transfer pathways being different, their amplitude depends on the quadrupolar coupling and crystallite orientation. For a powdered sample it is, thus, impossible to reach a perfect equalization of these amplitudes.

Amplitude-modulated experiments: (b) z-filter experiments. To overcome these problems, Amoureux *et al.* (1996) adapted the z-filter experiment to MQMAS. In this three-pulse scheme the two hard pulses (excitation of the MQ coherences and conversion to 0Q coherences) are followed by a short delay during which the magnetization is stored along the z-axis as zero-quantum coherences and then transferred into observable 1Q coherences by selective π/2 pulse (Fig. 4a). The symmetrization of the echo and antiecho pathways during the two hard pulses

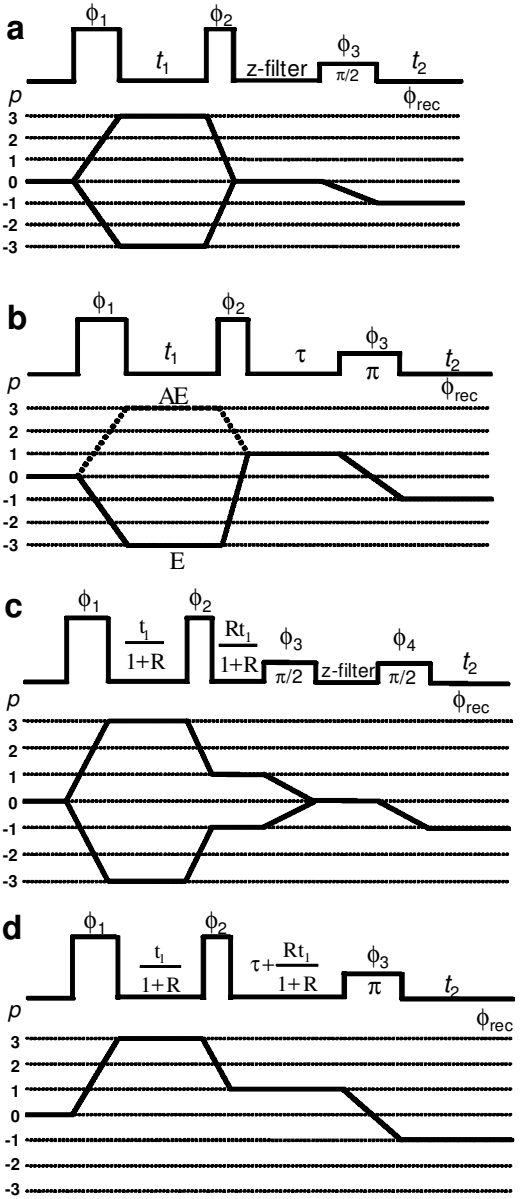

FIG. 4. Pulse sequences and coherence transfer pathways for 3QMAS NMR experiments. (a) Amplitude-modulated *z*-filter acquisition scheme. (b) Phase-modulated shifted-echo experiment for spin $I = 3/2$; E and AE represent, respectively, the echo and antiecho pathways. Split-t_1 (c) *z*-filter and (d) shifted-echo acquisition schemes for spin $I = 3/2$. ϕ_n represents the phase of pulse n. Phase cycling corresponding to these acquisition schemes can be found in the references where they were first described (see text).

($p = 0 \rightarrow \pm 3 \rightarrow 0$) forces an equal intensity of the echo and antiecho signals, leading to amplitude-modulated FIDs and, thus, to pure absorption spectra. This is a robust method which is easy to optimize.

Phase-modulated experiments: (a) shifted-echo or antiecho methods. The shifted-echo and antiecho methods use the properties of evenness and oddness of the time domain signals and their Fourier transforms, to eliminate the dispersive components from the 2D spectrum. The MQMAS shifted-echo experiment relies on the introduction of a refocusing π pulse at the end of the pulse sequence, in order to delay the formation of the echo (or antiecho) in the t_2 domain by a time τ (Fig. 4b). The latter delay must be long enough to avoid truncation of the signal at any t_1 value (whole-echo acquisition). Even though the time-domain signal is phase-modulated as in the original experiment proposed by Frydman and Harwood (1995), a complex two-dimensional transformation leads to a pure-phase spectrum, provided relaxation effects are negligible. Experimentally, since the echo forms at $t_2 = \tau$, rather than $t_2 = 0$ when $t_1 = 0$, a first-order phase correction must be applied in the F_2 dimension. Whole-echo acquisition, adapted to MQMAS by Massiot *et al.* (1996), may also be performed with the combination of shifted-echo and shifted-antiecho experiments, in order to increase the signal-to-noise ratio of the spectra. An amplitude-modulated signal is then obtained when the amplitudes of the shifted echo and shifted antiecho are equal. However, as a result of the properties of whole echoes, a hypercomplex two-dimensional Fourier transform still affords pure absorption lineshapes, even when the contributions of the two pathways are not equal.

Phase-modulated experiments: (b) split-t_1 experiments. As stated before, second-order broadened ridges appear in the MQMAS spectrum along the anisotropic axis A with direction $F_2 = R(I,p)F_1$. Therefore, the projection of this spectrum onto the F_1 axis is not isotropic. In order to obtain a two-dimensional spectrum with an isotropic F_1 projection, a shearing operation (explained in the section on analysis of MQMAS NMR spectra, below) has to be performed. An interesting alternative is the MQMAS split-t_1 experiment introduced by Brown *et al.* (1996), which splits t_1 into 1Q and MQ evolution periods in the proportion $R(I,p)$, refocusing the second-order anisotropic broadening at the end of the t_1 period. After a two-dimensional Fourier transform the anisotropic axis A appears parallel to the F_2 axis. This method may be combined with the z-filter or shifted-echo (whole-echo) schemes as shown in Fig. 4c and 4d, respectively (Brown & Wimperis, 1997), for 3Q MAS experiments on spin-3/2 nuclei. These schemes are easily extended to spins 5/2, 7/2 and 9/2 (Amoureux & Pruski, 2002). The four-pulse z-filter split-t_1 experiment is less efficient than the three-pulse shifted-echo split-t_1 experiment. The latter is probably the most efficient MQMAS scheme for spin-3/2 nuclei, in which the loss of magnetization due to T_2 effects is minor.

Analysis of MQMAS NMR spectra

Figure 5b shows the 'unsheared' (an explanation of shearing is given below) 3QMAS NMR spectrum of zeolite scolecite (which contains two non-equivalent four-coordinated Al sites) acquired with the three-pulse z-filter sequence. To assist the analysis of the spectrum, this figure also depicts the chemical shift (*CS*) axis, the anisotropic (*A*) axis and the quadrupolar-induced shift (*QIS*) axis. The slope of the *CS* axis is $-p$ and 1, when scales are in Hz or in ppm, respectively. Axis *A* is defined by the orientation of the anisotropic ridges in the spectrum and has slope $R(I,p)$. The centre of gravity of a given resonance is shifted from the *CS* axis, in both dimensions, by the *QIS*. This shift occurs in the direction of the *QIS* axis, with slope ξ:

$$\xi(I,p) = -p\frac{4I(I+1) - 3p^2}{4I(I+1) - 3} \qquad (3)$$

One important result is that it is possible to separate resonances with similar isotropic chemical shifts but different quadrupole parameters. Because for a given (I,p) pair the induced quadrupolar shifts have a unique sign, all observed signals (except the spinning sidebands) appear on the same side of the *CS* axis. Factors R and ξ for all I and p values are available (Amoureux & Fernandez, 1998). Using these values it is possible to estimate directly from the MQMAS spectrum the isotropic chemical shift, δ_{iso}, and the second-order quadrupolar effect parameter (SOQE) of the NMR peaks:

$$\delta_{iso}(\text{ppm} = \frac{(\xi(I,p)\delta_{G2} - |p|\delta_{G1})}{\xi(I,p) - |p|} \qquad (4)$$

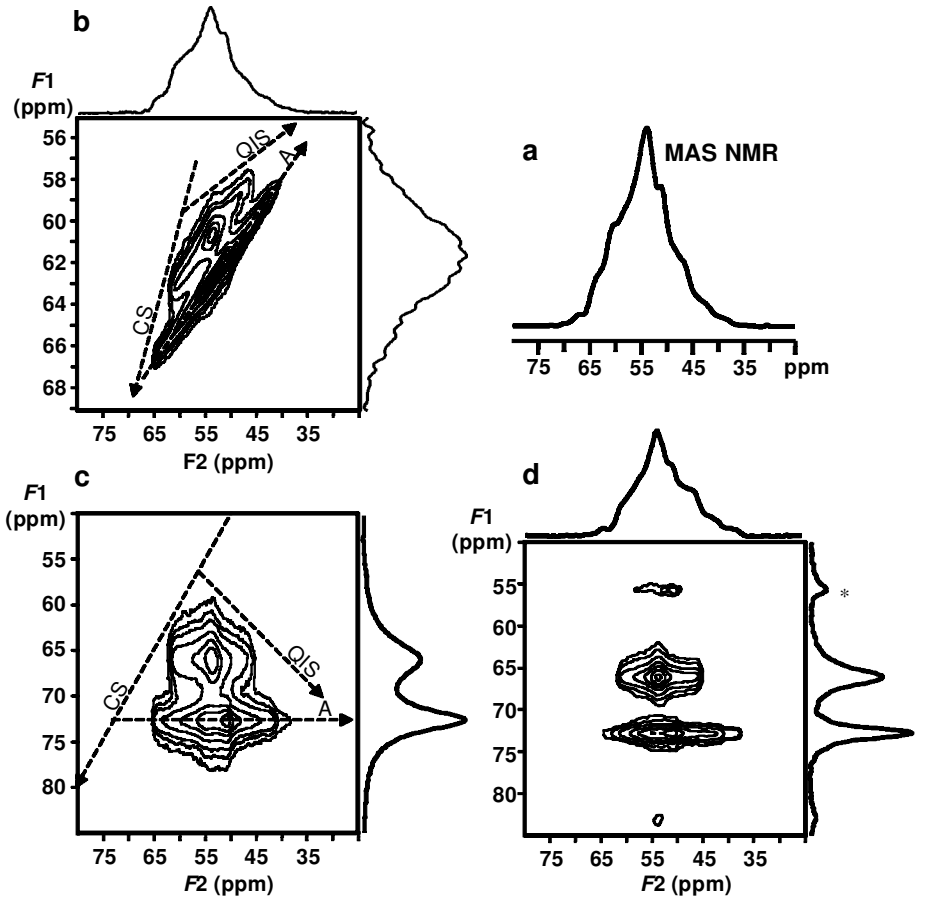

FIG. 5. (a) Single-quantum 'conventional', (b) unsheared and (c) sheared z-filter 3Q and (d) 5Q ^{27}Al MAS NMR spectra of zeolite scolecite recorded at 9.4 T. 'A', 'CS' and 'QIS' depict the anisotropic axis, chemical shift axis and quadrupolar-induced shift axis, respectively. The asterisk depicts a spinning sideband. 3QMAS spectrum was acquired with 3.6 μs and 1.1 μs pulse lengths for the first and second hard pulses, respectively (B_1 = 100 kHz). The soft pulse (B_1 = 6 kHz) length was 16 μs. 150 data points (96 transients per point) were acquired in the t_1 dimension in increments of $(1/\nu_r)$ = 80 μs. The ppm scale is referenced to ν_0 in the F_2 domain and to 1.42 ν_0 and 3 ν_0 in the F_1 domain, respectively, for the sheared and unsheared spectra (reference aqueous Al $(NO_3)_3$). The 5QMAS spectrum was acquired with 4.1 μs and 1.05 μs lengths for the first and second hard pulses, respectively (B_1 = 220 kHz). The soft pulse (B_1 = 8 kHz) length was 16 μs. 100 data points (880 transients per point) were acquired in the t_1 dimension in increments of $(1/4\nu_r)$= 20 μs. The ppm scale of the 5QMAS spectrum is referenced to ν_0 in the F_2 domain and to 7.08 ν_0 in the F_1 domain (reference aqueous Al $(NO_3)_3$).

$$(\mathrm{SOQE})^2(\mathrm{MHz}) = \mathrm{C}_\mathrm{Q}^2\left(1+\frac{\eta^2}{3}\right) = \frac{(\delta_{G2}-\delta_{iso})}{6000}\nu_0^2 \quad (5)$$

where δ_{G2} and δ_{G1} are the centres of gravity of the resonance along F_2 and F_1. Thus, the quadrupolar coupling constant, C_Q, may be determined provided the asymmetry parameter, η_Q, is known (this parameter may be obtained from simulation of the MAS NMR lineshape).

As stated before, one practical drawback of unsheared MQMAS NMR spectra is that its projection onto the F_1 axis is not isotropic. This is clearly shown in Fig. 5b where the F_1 projection does not resolve the two ^{27}Al NMR scolecite resonances. Hence, it is convenient to apply a shearing transformation to the MQMAS spectrum,

i.e. a mathematical operation which makes the A axis parallel to the F_2 axis. The F_1 projection of the 'sheared' spectrum is now isotropic and highly resolved, as shown in Fig. 5c, while the F_2 projection is essentially the 'conventional' (1Q) MAS NMR spectrum (Fig. 5a). The ppm scale in the F_1 dimension is referred to $\frac{R(I,p)-p}{R(I,p)-1}\nu_0$. Cross sections of the different resonances taken along F_2 can be used for the determination of C_Q and η_Q and the isotropic chemical shift is now given by:

$$\delta_{iso}(\text{ppm}) = \frac{(R(I,p) - |p|)\delta_{G1} - (R(I,p) - \xi(I,p))\delta_{G2}}{\xi(I,p) - |p|} \quad (6)$$

Figure 5 also compares the 3Q (5c) and 5QMAS (5d) spectra. Clearly, the latter is better resolved and, thus, despite the lower signal intensity, it is sometimes useful to record 5QMAS (and 7QMAS) spectra.

As another example, Fig. 6 shows the sheared 3QMAS NMR spectrum of AM-1, a synthetic layered Na titanosilicate. This is a particularly simple system because it contains a single type of Na ion. The 'conventional' ^{23}Na MAS NMR spectrum of AM-1 is shown in Fig. 6 and it resembles the F_2 projection of the 3QMAS NMR spectrum. The two peaks observed are, of course, not ascribed to two different Na sites, rather they are part of a second-order quadrupole powder pattern given by the single Na environment present in AM-1. In contrast, the F_1 projection of the 3QMAS NMR spectrum is not broadened by the second-order quadrupole interaction and exhibits a single, symmetric, peak. However, we stress, the centre of gravity of this projection is still shifted by the second-order quadrupole shift and, thus, the peak summit moves when the external magnetic field is changed.

AM-4 is another example of a synthetic layered Na titanosilicate material. The ^{23}Na MAS NMR spectrum of AM-4 (Fig. 7) displays a broad peak ranging from ~30 to −40 ppm, showing several singularities. The resolution of the 3QMAS NMR spectrum F_1 projection is very high, exhibiting at least nine peaks (Fig. 7). In particular, one of the resonances (~36 ppm F_1) is separated out from the main group of peaks by some 20 ppm. The quadrupole coupling parameters and the isotropic chemical shift of individual resonance may be obtained by simulating the cross-sections taken through each peak and parallel to F_2 (three examples are depicted in Fig. 7).

Consider cross-section A taken at 36 ppm in F_1. While along F_2 this peak spans some 45 ppm, along F_1 its full-width-at-half-maximum (FWHM) is only ~2 ppm. This is because this resonance is given by a Na site with a relatively large quadrupole coupling constant, revealed by simulation to be 2.6 MHz (η_Q = 0.82). In contrast, cross-sections B and C are narrower along F_2, corresponding to smaller quadrupole coupling constants of 2.1 and 1.6 MHz, respectively.

For highly crystalline solids, such as AM-4, the MQMAS NMR resonances are in general very narrow along F_1, but this not the case for disordered or amorphous materials. Indeed, in the latter, distributions of bond angles and bond lengths are

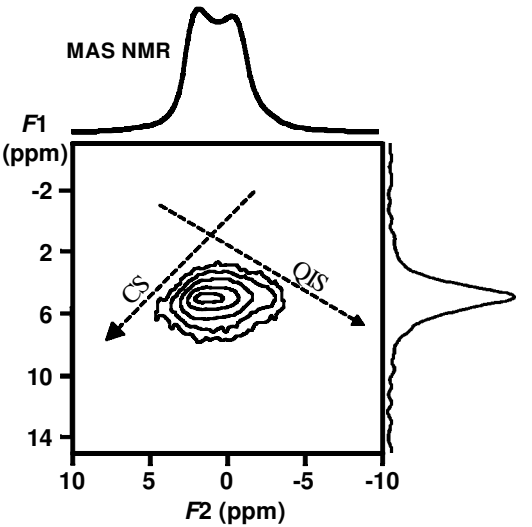

FIG. 6. Sheared ^{23}Na 3QMAS NMR spectrum of layered Na titanosilicate AM-1 recorded at 11.7 T. The single-quantum MAS NMR spectrum is shown instead of the (very similar) F_2 projection. 'CS' and 'QIS' depict, respectively, the chemical shift axis and quadrupolar-induced shift axis. The F_1 projection is isotropic, showing a single peak. The lengths of the first and second hard pulses were 7.1 μs and 2.3 μs, respectively (B_1 = 90 kHz). The soft pulse (B_1 =10 kHz) length was 12 μs. 64 data points (480 transients per point) were acquired in the t_1 dimension in increments of $(1/\nu_r)$ = 68.9 μs. The relaxation delay was 1.5 s. The ppm scale is referenced to ν_0 in the F_2 domain and to $3.78\nu_0$ in the F_1 domain (reference aqueous 1 M NaCl).

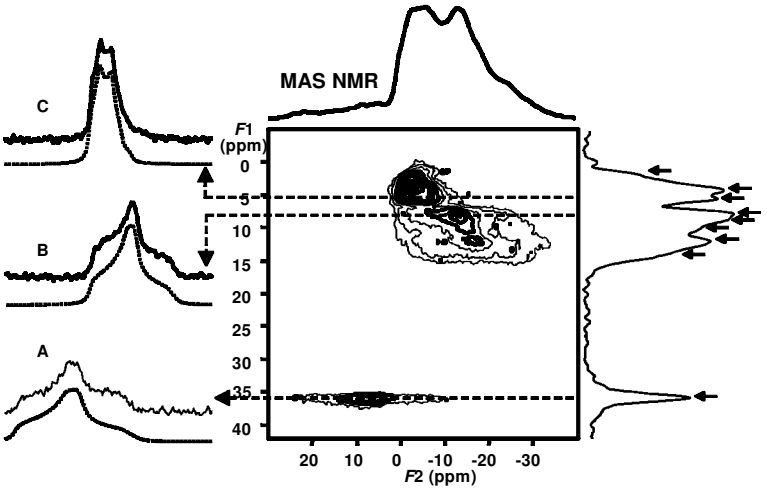

FIG. 7. Sheared ^{23}Na 3QMAS NMR spectrum of layered Na titanosilicate AM-4 recorded at 9.4 T. The single-quantum MAS NMR spectrum is shown instead of the (very similar) F_2 projection. Experimental (solid lines) and simulated (dashed lines) cross-sections taken parallel to the F_2 axis for three selected resonances (A, B, C) are given on the left of the 2D spectrum. The arrows depict the nine resonances present. The lengths of the first and second hard pulses were 2.5 μs and 0.8 μs, respectively (B_1 = 250 kHz). The soft pulse (B_1 = 9 kHz) length was 13 μs. 120 data points (480 transients per point) were acquired in the t_1 dimension in increments of $(1/\nu_r)$ = 31.25 μs. The recycle delay was 1.5 s. The ppm scale is referenced to ν_0 in the F_2 domain and to 3.78 ν_0 in the F_1 domain (reference aqueous 1 M NaCl).

present, resulting in dispersions of isotropic chemical shifts and quadrupole parameters, which may considerably broaden the lines along axes *CS* and *QIS*, respectively. For example, the AM-1 peak is broadened along the *CS* axis suggesting a slight distribution of the isotropic chemical shift (Fig. 6). As a result, the FWHM of the single-quantum ^{23}Na MAS NMR peak and F_1 projection are ~4.2 and 2.0 ppm, respectively, and, thus, the latter is not much narrower than the former. The relatively poor resolution of the MQMAS NMR spectra of glasses and other amorphous materials is, hence, not due to a limitation of the technique but is intrinsic to the material.

Quantification of MQMAS NMR spectra

An outstanding problem of MQMAS NMR spectroscopy is the quantification of the different resonances present. In general, the intensity (area) of resonances is not representative of the actual concentrations of the chemical species because the excitation (and conversion) of multiple-quantum coherences is strongly dependent on the NMR quadrupole frequency, pulse lengths and radio-frequency magnetic field amplitude (B_1).

The most accurate way of calculating site populations is by simultaneous simulation of the single-quantum and the full two-dimensional MQMAS NMR spectra (including distribution of quadrupole coupling parameters and isotropic chemical shifts, if present) using a programme that takes into account the efficiency of the MQMAS experiment as a function of the quadrupolar parameters (Fernandez *et al.*, in press). This is, however, not a trivial procedure and cannot be done routinely. When both a small number (say 2–4) of resonances are present in the MQMAS NMR spectrum, and there is little distribution of parameters, it is possible to calculate the peak intensities in a simpler way. Firstly, the (average) quadrupole parameters and isotropic chemical shift of each resonance are extracted from, e.g. the MQMAS NMR F_2 cross-sections. Then, these parameters are used to simulate the quantitative 1Q MAS NMR spectrum. This is a relatively straightforward procedure (particularly when the spectrum is partially resolved or displays singularities), performed with (freely) available software (Massiot *et al.*, 2002). When a large number of resonances overlap it may not be possible to calculate the relative intensities using this strategy.

In this case, quantitative information may still be obtained from the MQMAS spectrum by calculating the efficiency for the MQMAS experiment as a function of the quadrupolar parameters previously obtained by simulation of the F_2 cross sections of the MQMAS spectrum. This can be done using programmes such as PULSAR (Amoureux *et al.*, 1995), GAMMA (Smith *et al.*, 1994) and SIMPSON (Bak *et al.*, 2000).

MQMAS related experiments: STMAS and I-STMAS

Recently, Gan (2000) proposed a new, ingenious technique, known as Satellite Transition (ST) MAS NMR spectroscopy, which affords nearly quantitative spectra (at least for a large range of quadrupole coupling constants). In this experiment single-quantum satellite transitions (ST, $m = \pm 1/2 \rightleftharpoons m = \pm 3/2$, $m = \pm 3/2 \rightleftharpoons m = \pm 5/2$, etc.), rather than the symmetric multiple-quantum transitions (as in MQMAS), are correlated with the central transition (CT, $m = -1/2 \rightleftharpoons m = +1/2$) in a two-dimensional experiment performed under MAS. The CT is inherently free from first-order quadrupolar broadening, while a combination of MAS and rotor-synchronized acquisition removes ST first-order broadening. Under MAS, the residual CT and ST second-order quadrupolar broadenings differ by a scale factor only and, thus, it is possible to refocus the second-order broadenings in a two-dimensional correlation experiment. The creation of isotropic echoes occurs, therefore, in a similar fashion to the MQMAS experiment, though with much higher efficiency because coherence transfers occur only on the 1Q levels. An example (Amoureux *et al.*, 2003) of an ^{27}Al STMAS NMR spectrum (of zeolite scolecite) is shown in Fig. 8a.

Another method related to STMAS, Inverse (I) STMAS was described by Amoureux *et al.* (2003). I-ST MAS also correlates central and satellite coherences but does it in a reverse manner: CT evolves during the t_1 period while STs are detected during t_2 (Fig. 8b). The main limitation of the STMAS and I-STMAS experiments lies in the fact that they are technically demanding, requiring very accurate magic-angle setting (0.005º) and stable sample spinning (1–2 Hz) to average out the large ST first-order quadrupole interactions. A version of the STMAS experiment that Self-Compensates for Magic-Angle mis-sets (SCAM-STMAS) of up to 1º was recently proposed by Ashbrook & Wimperis (2002). However, the sensitivity of this experiment decreases when compared with standard STMAS. The latter and I-STMAS have other serious drawbacks restricting their application. Firstly, the spectral width along F_1 (STMAS) or F_2 (I-STMAS) is limited by the spinning rate. Secondly, both methods are very sensitive to any molecular motion, which leads to short transverse relaxation times and, consequently, to a large signal decrease and degradation of isotropic resolution (Ashbrook *et al.*, 2002).

Detection of resonances with large quadrupole couplings

When resonances with large quadrupole coupling constants are present, the MQMAS experiment is fairly inefficient, even when using the largest

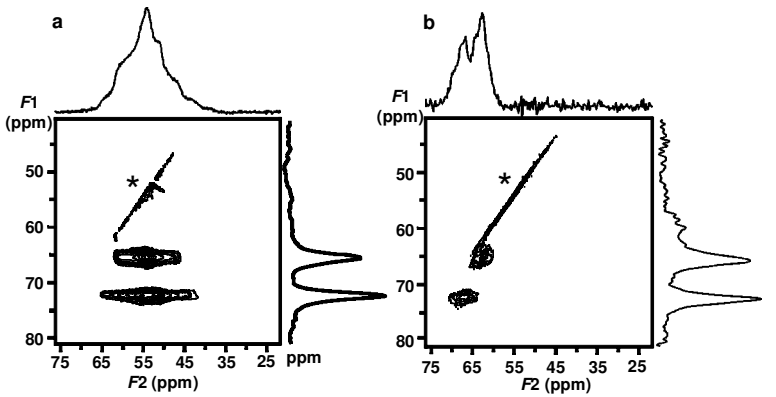

FIG. 8. Sheared ^{27}Al (a) STMAS, (b) I-STMAS NMR spectra of zeolite scolecite recorded at 9.4 T with a MAS rate of 12.5 kHz, using soft (5 kHz) and hard (50 kHz) pulses (see Amoureux *at al.*, 2003, for experimental details). Asterisks depict CT-CT signals not completely cancelled out.

available B_1 fields (~250 kHz). In extreme cases (relatively low B_1 and large quadrupole couplings), the peak intensity may be so low that the resonance remains buried in the noise and is not detected. Ding & McDowell (1997) and Marinelli *et al.* (1998) showed that 3Q excitation in spin-3/2 systems could be improved by using shaped or composite pulses, respectively, instead of CW irradiation. However, the gains achieved are not appreciable (intensity gain of up to 30% was reported under relatively slow spinning conditions). This is because the poor signal-to-noise ratio of the MQMAS experiment is mainly due to the inefficiency of the conversion of MQ to 1Q coherences. In order to deal with this problem some successful modifications of the MQMAS NMR experiment, that are less sensitive to C_Q and thus extend to larger values the range of quadrupolar couplings that are accessible to MQMAS, were reported.

Based on the work of Vega (1992), Wu *et al.* (1996) proposed RIACT, a technique which employs rotation-induced adiabatic coherence transfer between 3Q and 1Q coherences in spin-3/2 systems under MAS. The excitation consists of a selective 90º pulse, immediately followed by a long (1/4 of the rotor period) hard pulse; in the conversion step a long hard pulse of the same duration is also used. Although more quantitative, RIACT MQMAS spectra present distorted lineshapes along the MAS dimension and the position of the r.f. offset substantially affects its efficiency (Lim & Grey, 1998). Caldarelli & Ziarelli (2000) showed that this approach can be used to selectively excite certain sites according to their quadrupolar constants while minimizing the intensity of others and, thus, it may be used as a spectral editing technique.

The DFS (Double Frequency Sweeps) and FAM (Fast Amplitude Modulation) methods introduced by Kentgens & Verhagen (1999) and Madhu *et al.* (1999), respectively, achieve significant sensitivity enhancements by using modulated, instead of continuous wave (CW), pulses for the conversion of MQ to 1Q coherences. Both methods rely on selective irradiation of the satellite transitions, following the idea introduced by Vega & Naor (1981) for the 3Q to 1Q conversion in single crystals of spin-3/2 nuclei. Although these methods are based on similar physical principles, their experimental implementation is quite different. DFS sweeps the r.f.-carrier frequency over the entire satellite spectrum, while FAM corresponds to irradiation at two distinct frequencies, ideally on the singularities of the satellite powder pattern. The latter is of special interest because it is easy to implement in standard NMR spectrometers. Like RIACT, FAM (often referred to as FAM-I) and DFS methods, initially introduced for spin-3/2-nuclei, use adiabatic energy level anti-crossings in order to efficiently convert the 3Q into 1Q coherences (Madhu *et al.*, 2000; Schäfer *et al.*, 2000). Their major advantage over RIACT is the improved lineshapes along the anisotropic dimension.

Fast amplitude modulation allows the redistribution of the population of the spin energy levels. This is the rotor-assisted population transfer (RAPT) method introduced by Yao *et al.* (2000). It has been shown that an enhancement by a factor of 1.5–2 is achieved in a MAS experiment of spin-3/2 nuclei when RAPT is applied before the excitation pulse. It is also possible to combine RAPT with a MQMAS experiment that used single-quantum coherences for the excitation of MQ coherences. Madhu & Levitt (2002) have shown that a combination of RAPT with RIACT-FAM gives the best performance for MQMAS experiments of spin-3/2 systems.

Although Vosegaard *et al.* (2000) reported sensitivity enhancements of 3QMAS and 5QMAS spectra of $I = 5/2$ nuclei using FAM-I pulses, this approach is not well suited for these spin systems. To improve 3QMAS spectra of spin-5/2 nuclei Goldbourt *et al.* (2000) introduced FAM-II pulses, which are built of a set of equal intensity segments with alternating positive and negative phases. The success of FAM-II pulses depends on the quadrupolar frequency parameters of the sample and on the length and intensity of the pulse segments, both determined numerically or experimentally. In contrast with FAM-I, FAM-II pulses do not contain zero intensity delays and the lengths of the segments are different. The MQ to SQ coherence transfer mechanism during FAM-II pulses is not thought to be adiabatic, but rather is a cumulative direct process. Morais *et al.* (2003) reported a different optimization strategy for the FAM-II MQ MAS experiment that further improves the multiple to single-quantum transfer efficiency.

The ^{27}Al FAM-II 3QMAS NMR spectrum of kaolinite partially decomposed to (highly disordered) metakaolinite by calcination in air at 550ºC (Fig. 9a) exhibits resonances attributed to tetra-

(~85 ppm F_1), penta- (~45 ppm F_1) and hexacoordinated (~5 ppm F_1) Al (Morais *et al.*, 2003). In the latter, peaks from kaolinite and metakaolinite overlap. Figure 9b compares the F_1 and F_2 projections of the CW and FAM-II MAS NMR spectra. Clearly, the tetra- and penta-coordinated Al resonances are much enhanced when using the FAM-II technique. This is because they are given by metakaolinite distorted Al sites with relatively large quadrupole coupling constants, while the main contribution to the hexacoordinated Al peak is that of kaolinite.

Another approach to obtain sensitivity enhancement in MQMAS experiments of spin-3/2 systems was suggested by Vosegaard *et al.* (2001). The proposed experiment called FASTER (FAst Spinning gives Transfer Enhancement at Rotary Resonance) exploits a rotary resonance between the r.f. field amplitude (ν_1) and the spinning rate (ν_r) at high MAS rates and low r.f. field amplitudes. 3Q excitation efficiency is enhanced when ν_r and ν_1 are between adjacent rotary resonance conditions ($\nu_1 = n\nu_r/2$) and the 3Q to 1Q conversion is enhanced when $\nu_1 = n\nu_r$. As with RIACT, FASTER MQMAS spectra present distorted lineshapes along the anisotropic dimension.

Additional gain in the signal-to-noise ratio can also be obtained by synchronous detection (Massiot, 1996) or by acquiring multiple echoes during the free precession period of the observable single-quantum 1Q (MQ-QCPMG-MAS experiment proposed by Vosegaard *et al.*, 1997). The latter technique is only applicable when T_2 relaxation is not too fast.

When the quadrupolar couplings are so large that at normal field strengths and spinning rates the MAS spectrum is too complicated because of the overlap of the numerous spinning sidebands, it becomes impossible to record MQMAS spectra. Massiot *et al.* (1997) showed that in such cases the spinning sidebands can be separated by order in a two-dimensional experiment from which it is possible to obtain an infinite spinning rate (spinning-sideband free) MAS spectrum. The proposed experiment called QPASS (quadrupolar phase adjusted spinning sidebands), provides MAS spectra with enhanced

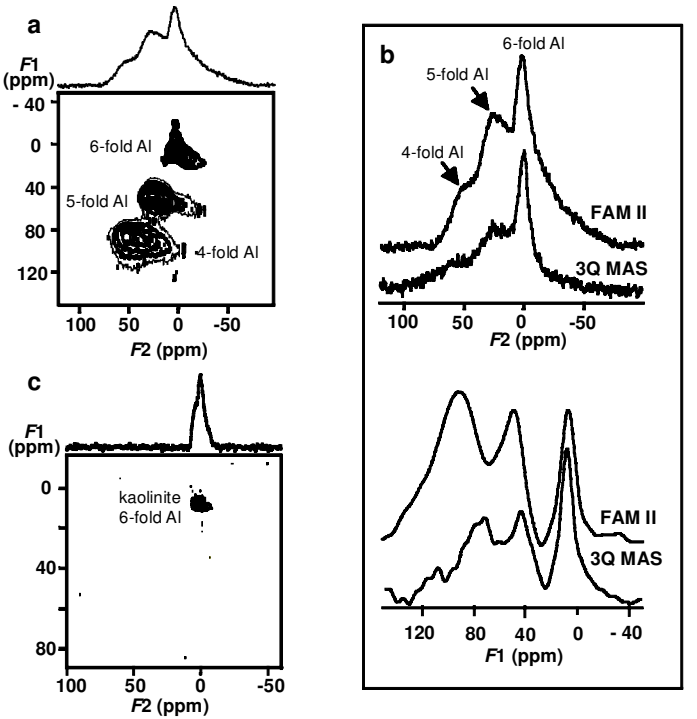

FIG. 9. ^{27}Al (a) FAM-II 3QMAS, (b) CW and FAM-II F_1 (isotropic) and F_2 projections, and (c) ^{1}H→^{27}Al cross-polarization spectra of kaolinite calcined at 500°C for 1 h, recorded at 9.4 T with a 15 kHz spinning rate and a 1s recycle delay (see Morais *et al.*, 2003, for experimental details).

resolution enabling the extraction of quadrupolar parameters and isotropic chemical shifts. The method has been applied to several materials containing ^{71}Ga, including two layered Ga hydrophosphonates (Massiot *et al.*, 1999).

DOUBLE RESONANCE EXPERIMENTS

Spectral editing and MQMAS

Combining ^{1}H (or ^{19}F)→^{27}Al cross-polarization (CP) with MQMAS NMR affords a powerful method for simplifying spectra, helping in the attribution of resonances. In the CP-MQMAS experiment introduced by Pruski *et al.* (1997) the spin *I* (spin-1/2 nucleus) magnetization is transferred into the 1Q coherence of spin *S* (quadrupolar nucleus) employing a very low r.f. field on the quadrupolar spin channel. The resulting 1Q coherence is then converted into 0Q coherence by a selective pulse and, after a short delay, a standard MQMAS experiment is performed. An alternative approach for combining cross-polarization with MQMAS has been proposed by Ashbrook & Wimperis (1998). In this method, the quadrupolar spin MQ coherences are created directly by cross-polarization. This more direct and efficient approach was also used by Lim & Grey (1999) and Rovnyak *et al.* (2000). The possibility of direct cross-polarization of higher-order MQ coherences was shown by Ashbrook & Wimperis (2000). Another method, proposed by these authors (Ashbrook & Wimperis, 2001), combines 1Q cross-polarization with a reversed split-t_1 MQMAS experiment, where the 1Q coherences are transferred directly to 3Q coherences, rather than via a population state. This results in a pulse sequence with a minimum number of coherence transfer steps. Furthermore, the authors showed that the sensitivity of the experiment may be considerably improved by incorporating FAM pulses in the MQ excitation and MQ to 1Q conversion steps.

As an example, consider again the spectra of partially decomposed kaolinite recorded with and without cross-polarization (Fig. 9a,c). Because the remaining parent (non-decomposed) kaolinite is much richer than metakaolinite in hydroxyl groups, the ^{1}H→^{27}Al CP 3QMAS NMR spectrum displays only the hexacoordinated Al resonance given by the former or, in other words, the metakaolinite peaks are filtered out of the spectrum.

As the spin-dynamics of the CP transfer involving quadrupolar nuclei is very complex, CP-based methods may suffer from quantitative uncertainties. An alternative for spectral editing without the use of CP is the MQ-REDOR experiment introduced by Fernandez *et al.* (1998). This method relies on reintroducing the heteronuclear dipolar dephasing between spins using rotor-synchronized r.f. pulses, which are applied during the 1Q evolution (MQ-t_2-REDOR) of a MQMAS experiment. Furthermore, this technique allows the measurement of distances between quadrupolar and spin-1/2 nuclei. Pruski *et al.* (1999) showed that the application of REDOR recoupling pulses during 3Q, rather than 1Q evolution (MQ-t_1-REDOR), enhances the dipolar interaction by a factor of three and, thus, has potential for improving sensitivity in weak coupled spins.

Heteronuclear correlation MQMAS spectroscopy

Heteronuclear-correlation (HETCOR) MQMAS spectra afford a very useful method for studying connectivity between spin-1/2 and quadrupolar nuclei. This technique was demonstrated for spin-3/2 by Wang *et al.* (1997) with a spectrum correlating the isotropic resonances of ^{23}Na (spin 3/2) and ^{31}P (spin 1/2) in $Na_3P_3O_9$. Several schemes have been proposed to obtain similar spectra for spin-5/2 nuclei. Fernandez *et al.* (2001) showed that these schemes resulted in distorted spectra and that an extension of the experiment introduced by Wang *et al.* should be used instead. The same authors (Fernandez *et al.*, 2002) demonstrated the 5Q version of the experiment.

Delevoye *et al.* (2003) showed that low-power ^{27}Al decoupling may be used to remove residual J-coupling interactions between ^{31}P and ^{27}Al in some aluminophosphates. Used in tandem with ^{1}H high-power decoupling, ^{27}Al decoupling greatly improves the resolution of ^{31}P MAS and ^{31}P→^{27}Al MQ HETCOR spectra. Figure 10 shows ^{31}P→^{27}Al MQ HETCOR spectrum of microporous aluminophosphate $AlPO_4$-14 (Delevoye *et al.*, 2003). No connectivity is observed for hexacoordinated Al(4) and P(1), tetracoordinated Al(3) and P(2), and tetracoordinated Al(2) and P(3). Pentacoordinated Al(1) exhibits connectivity between all four P sites. These results are in accord with crystallographic evidence.

Indirect detection of quadrupolar nuclei

New opportunities to detect nuclei with large quadrupolar coupling constants rely on the detection of weak dipolar couplings between these nuclei and a spin 1/2-nucleus, such as ^{1}H. For non-spinning solids, the dipolar couplings can be measured using Spin-Echo Double and Resonance (SEDOR) (Wang *et al*., 1984). However, MAS-based methods are superior because they lead to the observation of the spin-1/2 nuclei under high-resolution conditions. The heteronuclear dipolar interaction, averaged to zero by MAS, can be reintroduced by the Rotational Echo DOuble Resonance (REDOR) (Gullion & Schaefer, 1989) and TRAnsfer of Population in DOuble Resonance (TRAPDOR) (Van Eck *et al*., 1990; Grey & Vega, 1995) experiments. Rotational Echo Adiabatic Passage Double Resonance (REAPDOR) (Gullion, 1995) is a new technique for recovering the dipolar interaction between an observed $S = 1/2$ and a dephased $I > 1/2$ spin pair. This method is a combination of the REDOR and TRAPDOR MAS experiments when applied to heteronuclear spin pairs. In addition to the spectral editing potential of these techniques, they offer the possibility of determining, indirectly, the quadrupolar coupling constants of the non-observed quadrupolar spin (Grey & Vega, 1995). This is achieved by continuously varying the irradiation frequency offset on the quadrupolar nuclei. When this frequency is in the range of the satellite transition powder pattern of the quadrupolar spin the dipolar dephasing is not null; when it reaches the edges of the satellite transition the dipolar dephasing effect vanishes. This allows the indirect determination of the satellite transition and thus the magnitude of the quadrupolar interaction.

MQMAS NMR STUDIES OF LAYERED MATERIALS

Silicates

Hanaya & Harris (1998) studied the local coordination environment of Na ions in the interlayer spaces of hydrous layered silicates with empirical formulae $Na_2O{\cdot}(4-20)SiO_2{\cdot}(5-10)H_2O$, makatite, kanemite, octosilicate, magadiite and kenyaite. Highly-resolved ^{23}Na 3QMAS NMR spectra of makatite, $Na_2Si_4O_8(OH)_2{\cdot}4H_2O$, were

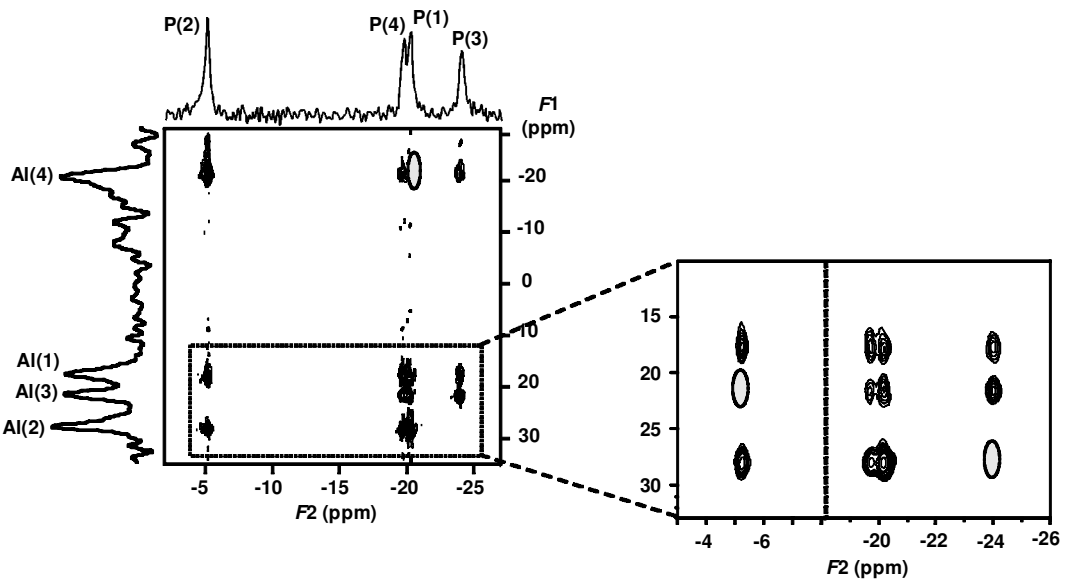

FIG. 10. $^{31}P \rightarrow {}^{27}Al$ MQ HETCOR spectrum of microporous aluminophosphate $AlPO_4$-14 acquired using the pulse sequence described by Fernandez *et al*. (2002). The spectrum was recorded at 9.4 T with a 10 kHz spinning rate and 1 s recycle delay. The lengths of the pulses for triple-quantum excitation and for triple to single-quantum conversion were 3.4 μs and 1.5 μs, respectively. Efficient cross-polarization was achieved for a ^{31}P rf field of 30 kHz and a ^{27}Al r.f. field of 6 kHz. The contact time was 2 ms. ^{1}H/^{27}Al double-resonance decoupling was applied during the acquisition time. The r.f. decoupling fields were 90 and 12 kHz for ^{1}H and ^{27}Al, respectively.

only obtained when high-power ^{1}H decoupling was used (Hanaya & Harris, 1997; Hayashi, 1997). The three resonances observed are in accord with the single-crystal XRD structure (only available for makatite), which calls for the presence of three types of Na ions. The ^{23}Na NMR evidence indicates that the makatite structure is not directly related to those of the other layered silicates studied. For example, all Na ions in the latter materials are thought to be in octahedral coordination, while in makatite, two Na ions are coordinated by six water oxygens, the other being coordinated by two water oxygens and three silanol oxygens. A tendency for larger chemical shifts (δ_{iso}) for pentacoordinated than for hexacoordinated Na ions was observed, suggesting the possibility of using δ_{iso} to distinguish the coordination number of Na ions, at least in this type of compound.

Rocha *et al.* (1999) investigated by powder XRD and ^{27}Al 3QMAS NMR the reconstruction of layered double hydroxides with the hydrotalcite structure from materials previously calcined at increasing temperatures and different rehydration times. The parent sample contains two types of hexacoordinated Al sites (peak with shoulder at ~9 ppm), one of which exhibits a distribution of isotropic chemical shifts, attributed to the presence of a range of slightly different local Al environments generated by the random insertion of Al in the layers. When the sample is calcined at 250ºC, the ^{27}Al MAS NMR peak broadens indicating that the structure becomes increasingly disordered. About 25% of Al ions migrate from octahedral to tetrahedral coordination (peak at 76 ppm), giving rise to cation vacancies in the layer. At 350ºC and above the structure undergoes major changes, which are closely monitored by ^{27}Al 3QMAS NMR. It was found that reconstruction is complete after 24 h of rehydration when the sample had been calcined to 550ºC, while equilibration for 3 days is adequate to reconstruct samples calcined at 750ºC. Only partial reconstruction occurs after calcinations at 1000ºC.

Lee & Stebbins (2003) reported ^{17}O 3QMAS NMR spectra of ^{17}O-enriched natural kaolinite and muscovite that provide improved resolution of the signal for the apical oxygens and, in particular, three crystallographically distinct basal oxygen sites in kaolinite, providing further insight into the origin of possible reactivity differences among the sites. Lee *et al.* (2003) studied by ^{17}O and ^{27}Al 3QMAS NMR ^{17}O-enriched synthetic layered materials and natural kaolinite and muscovite. Basal and apical oxygen sites have well-defined ranges of ^{17}O isotropic chemical shifts and quadrupolar coupling constants. The C_Q of basal oxygen (Si-O-Si) ranges from 4.1 to 5.2 MHz for these phases, while δ_{iso} varies from 39 to 55 ppm. The δ_{iso} value of basal oxygen sites increases with increasing C_Q. The C_Q and δ_{iso} values of apical oxygens (Si-O-hexacoordinated Al) are ~3.4 MHz and 64 ppm, respectively, and were similar among the phases studied. The hydroxyl group (2 hexacoordinated Al-OH) exhibited the largest C_Q (~7 MHz) among the oxygen sites and δ_{iso} in the range 37–44 ppm.

The kaolinite-mullite reaction process was revisited by single- and triple-quantum ^{27}Al MAS NMR (Rocha, 1999). It was shown that in order to record reliable spectra it is important to use very fast (in excess of 30 kHz) sample spinning rates. In accord with previously established knowledge, it was found that the decomposition of kaolinite begins at ~500ºC and is essentially complete at ~600ºC. Dehydrated kaolinite, metakaolinite, is metastable up to ~900ºC. ^{27}Al 3QMAS NMR provides solid evidence for the presence in metakaolinite of a dispersion of distorted tetra, penta and hexacoordinated Al local environments, typical of a disordered material. The quantification of the populations of these sites is a non-trivial task and remains an unsolved problem.

Ashbrook & Wimperis (2000) studied by ^{27}Al MAS NMR kaolinite, gibbsite and mixtures of the two which were ground together for varying times. Cross-polarization techniques were used for editing the two-dimensional 3QMAS NMR spectra, thereby allowing overlapping peaks corresponding to hexacoordinated Al sites to be studied. Mechanical treatment of the kaolinite-gibbsite mixture for a short period does not produce any significant structural changes. More extended grinding of these mixtures leads to substantial changes in structure and the formation of new Al sites with varying coordination numbers.

Delevoye *et al.* (2003) investigated, by ^{1}H, ^{23}Na, ^{27}Al and ^{29}Si MAS NMR, laponite and a range of synthetic saponites of variable interlayer charge. A single ^{27}Al NMR resonance was observed for all saponite samples whose linewidth increases with the clay charge. One well-defined ^{23}Na NMR resonance (whose isotropic chemical shift evolves progressively with the clay charge) is observed for all materials studied, except the highest-charged saponite, which exhibits at least two distributed peaks.

The hydration process of layered Na disilicate SKS-5 was studied by a range of techniques including ^{23}Na MAS NMR (Ai *et al.*, 2002). SKS-5 is gradually converted from α-$Na_2Si_2O_5$ to a new, poorly characterized, phase during hydration. The coordination of Na ions changes considerably during hydration. Five Na sites were detected by ^{23}Na MAS and 3QMAS NMR and their attribution is discussed.

Other layered materials

Microporous and layered aluminophosphates have been much studied by solid-state NMR because they possess two abundant NMR active nuclei, ^{27}Al and ^{31}P. However, while the latter is a spin-1/2 nucleus and yields, under MAS conditions, highly-resolved spectra, this is not the case with ^{27}Al, which requires the use of multiple-quantum MAS NMR to attain such resolution. One of the first layered aluminophosphates studied by ^{27}Al MQMAS NMR was a material templated by 1,8-diaminooctane (DAO) and known as AP2DAO, with formula $(C_8N_2H_{22})_8[Al_{13}P_{18}O_{72}]\cdot 6H_2O$ (Tuel *et al.*, 2001). The structure consists of layers built up of tetrahedrally coordinated Al and P atoms, separated by and hydrogen bonded to doubly protonated DAO molecules. One of the 13 Al atoms is hexacoordinated to 6 P tetrahedral forming $Al(OP)_6$ units which are responsible for the unusual (never reported earlier) layer stoichiometry (P:Al = 18:13). ^{27}Al 5QMAS NMR resolves the single hexacoordinated and the two tetracoordinated Al sites present and confirms the XRD crystal structure. The assignment of the Al resonances was assisted by ^{27}Al→^{31}P HETCOR NMR, although the lines along the ^{27}Al axis were broadened by the second-order quadrupole interaction (in other words the spectrum recorded was not a ^{27}Al→^{31}P MQ HETCOR).

The same authors reported three other examples of layered aluminophosphates. The structure of AP2pip, $(C_4N_2H_{12})_{4.5}[Al_3P_4O_{16}]_3\cdot 5H_2O$, is made up of sheets containing PO_4 tetrahedra linked to three AlO_4 tetrahedra in a strictly alternating fashion, the fourth bond being a P=O bond. These sheets consist of two chain types (A and B) running along [001] in the sequence AABAAB. The inorganic sheets are separated by and hydrogen bonded to doubly protonated piperazine molecules in two different orientations. Although the XRD crystal structure calls for the presence of nine non-equivalent Al sites, ^{27}Al 5QMAS NMR only resolves four (possibly five) distinct resonances, presumably because several atoms of the structure possess similar isotropic chemical shifts and quadrupole parameters (Tuel *et al.*, 2001). A second aluminophosphate, templated with 2-methylpiperazine, APMeP200, possesses a structure almost identical to the structure of AP2pip. Finally, APMep150, $(C_4N_2H_{14})_3(H_2O)_{10}$ $[Al_6P_8O_{32}(H_2O)_2]$, contains aluminophosphate layers consisting of a network of 4-, 6- and 12-membered rings, which are also observed in other previously reported layered aluminophosphates but differ here by the presence of a disordered Al octahedron in the unit cell (Tuel *et al.*, 2002). The subtleties of the structure are revealed by ^{27}Al 5QMAS NMR, which shows the presence of a single hexacoordinated and three tetracoordinated Al species, explained by assuming that the AlO_6 octahedra are locally ordered in the structure.

MQMAS NMR studies on a few other layered materials are available. For example, Fontenot *et al.* (2002) reported on ^{17}O MAS and 3QMAS NMR of layered $V_2O_5]\cdot nH_2O$ gels. The spectra were surprisingly complex and yielded much information on the structural information. In another work, Kanehashi *et al.* (2002) characterized the mineral materials in dry coals by ^{27}Al and ^{1}H→^{27}Al 3Q CP MAS NMR.

The advantages of recording NMR spectra of layered (and other) materials at very high (up to 21.1 T, 900 MHz ^{1}H frequency) magnetic fields were clearly demonstrated by Stebbins and co-workers. In particular, the authors reported ^{39}K spin-echo MAS NMR spectra of muscovite (Stebbins *et al.*, 2002). ^{39}K (I = 3/2) is perceived as a difficult nucleus for NMR studies mainly because of its low magnetogyric ratio, γ. High-field NMR was also used with much success by Lee *et al.* (2003) for studying kaolinite and muscovite.

CONCLUSIONS AND OVERVIEW

Multiple-quantum magic-angle spinning NMR is a powerful tool to study half-integer quadrupolar nuclei in solids. Since its introduction in 1995 MQMAS NMR has evolved considerably and, at present, a range of very useful related techniques is available. Despite the fact that the basic MQ MAS pulse sequences are robust and easily implemented in a conventional solid-state NMR spectrometer, a surprisingly small number of studies are available on layered materials, concentrating on ^{27}Al and, to

a lesser extent, ^{17}O and ^{23}Na. In the near future we expect to see a strong increase in the application of MQMAS NMR to the study of layered materials, particularly on natural specimens. We hope this review gives the reader an impetus in this direction.

REFERENCES

Ai X., Deng F., Dong J., Chen L. & Ye C. (2002) Stability of layered sodium disilicate during hydration process as studied by multinuclear solid state NMR spectroscopy. *Journal of Physical Chemistry*, **106**, 9237–9244.

Amoureux J.P. & Fernandez C. (1998) Triple, quintuple and higher order multiple quantum MAS NMR of quadrupolar nuclei. *Solid State Nuclear Magnetic Resonance*, **10**, 211–223.

Amoureux J.P. & Pruski M. (2002) Advances in MQMAS. Pp. 226–251 in: *Encyclopedia of Nuclear Magnetic Resonance* vol. **9** (D.M. Grant & R.K. Harris, editors). Wiley, Chichester, UK.

Amoureux J.P., Fernandez C. & Dumazy Y. (1995) A useful tool for the elaboration of new solid-state experiments: PULSAR. *Journal de Chimie Physique*, **2**, 1939– 1949.

Amoureux J.P., Fernandez C. & Steuernagel S. (1996) Z filtering in MQMAS NMR. *Journal of Magnetic Resonance A*, **123**, 116–118.

Amoureux J.P., Morais C., Trebosc J., Rocha J. & Fernandez C. (2003) I- STMAS, a new high-resolution solid-state NMR method for half-integer quadrupolar nuclei. *Solid State Nuclear Magnetic Resonance*, **23**, 213–223.

Ashbrook S.E. & Wimperis S. (1998) Multiple-quantum cross-polarization in MAS NMR of quadrupolar nuclei. *Chemical Physics Letters*, **288**, 509–517.

Ashbrook S.E. & Wimperis S. (2000) Multiple-quantum cross-polarization and two-dimensional MQMAS NMR of quadrupolar nuclei. *Journal of Magnetic Resonance*, **147**, 238–248.

Ashbrook S.E. & Wimperis S. (2001) Novel two-dimensional methods that combine single-quantum cross-polarization and multiple-quantum MAS of quadrupolar nuclei. *Chemical Physics Letters,* **340**, 500–508.

Ashbrook S.E. & Wimperis S. (2002) High-resolution NMR spectroscopy of quadrupolar nuclei in solids: Satellite-transition MAS with self-compensation for magic-angle Misset. *Journal of the American Chemical Society*, **124**, 11602–11603.

Ashbrook S., McManus J., MacKenzie K.J.D. & Wimperis S. (2000) Multiple-quantum and cross-polarized ^{27}Al MAS NMR of mechanically treated mixtures of kaolinite and gibbsite. *Journal of Physical Chemistry B*, **104**, 6408–6416.

Ashbrook S.E., Antonijevic S., Berry A.J. & Wimperis S. (2002) Motional broadening: an important distinction between multiple-quantum and satellite-transition MAS NMR of quadrupolar nuclei. *Chemical Physics Letters*, **364**, 634–642.

Bak M., Rasmussen J.T. & Nielsen N.C. (2000) SIMPSON: A general simulation program for solid-state NMR spectroscopy. *Journal of Magnetic Resonance*, **147**, 296–330.

Brown S.P. & Wimperis S. (1997) Two-dimensional multiple-quantum MAS NMR of quadrupolar nuclei: A Comparison of Methods. *Journal of Magnetic Resonance*, **128**, 42–61

Brown S.P., Heyes S.J. & Wimperis S. (1996) Two-dimesional MAS multiple-quantum NMR of quadrupolar nuclei. Removal of inhomogeneous second-order broadening. *Journal of Magnetic Resonance A*, **119**, 280–284.

Caldarelli S. & Ziarelli F. (2000) Spectral editing of solid-state MAS NMR spectra of half-integer quadrupolar nuclei. *Journal of the American Chemical Society*, **122**, 12015–12016.

Chmelka B.F, Mueller K.T., Pines A., Stebbins J., Wu Y. & Zwanziger, J.W. (1989) Oxygen-17 NMR in solids by dynamic-angle spinning and double-rotation. *Nature*, **339**, 42–43.

Delevoye L., Fernandez C., Morais C.M., Amoureux J.P., Montouillout V. & Rocha J. (2003) Double-resonance decoupling for resolution enhancement of ^{31}P solid-state MAS and $^{27}Al \rightarrow {}^{31}P$ MQHETCOR NMR experiments. *Solid State Nuclear Magnetic Resonance*, **21**, 61–70.

Delevoye L., Robert J.L. & Grandjean J. (2003) ^{23}Na 2D 3QMAS NMR and ^{29}Si, ^{27}Al MAS NMR investigation of Laponite and synthetic saponites of variable interlayer charge. *Clay Minerals*, **38**, 63–69.

Ding S. & McDowell C.A. (1997) Shaped-pulse excitation in multi-quantum magic-angle spinning spectroscopy of half-integer quadrupole spin systems. *Chemical Physics Letters*, **270**, 81–86.

Fenzke D., Freude D., Fröhlich T. & Haase J. (1984) NMR intensity measurements of half-integer quadrupolar nuclei. *Chemical Physics Letters*, **111**, 171–175.

Fernandez C., Lang D.P, Amoureux J.P. & Pruski M. (1998) Measurement of heteronuclear dipolar interaction between quadrupolar and spin 1/2 nuclei by MQ REDOR NMR. *Journal of the American Chemical Society*, **120**, 2672–2673.

Fernandez C., Morais C., Rocha J. & Pruski M. (2002) High-resolution correlation spectra between ^{31}P and ^{27}Al in microporous aluminophosphates. *Solid State Nuclear Magnetic Resonance*, **21**, 61–70.

Fontenot C.J., Wiench J.W., Schrader G.L. & Pruski M. (2002) ^{17}O MAS and 3QMAS NMR investigation of the crystalline V_2O_5 and layered $V_2O_5.nH_2O$ gels. *Journal of the American Chemical Society*, **124**, 8435–8444.

Frydman L. & Harwood J.S. (1995) Isotropic spectra of half-integer quadrupole spins from bidimensional magic-angle-spinning NMR. *Journal of the American Chemical Society*, **117**, 5367–5368.

Gan Z. (2000) Isotropic NMR spectra of half-integer quadrupolar nuclei using satellite transitions and MAS. *Journal of the American Chemical Society*, **122**, 3242–3243.

Goldbourt A., Madhu P.K. & Vega S. (2000) Enhanced conversion of triple to single-quantum coherence in the triple-quantum MAS NMR spectroscopy of spin-5/2 nuclei. *Chemical Physics Letters*, **320**, 448–456.

Grey C.P. & Vega A.J. (1995) Determination of the quadrupole coupling constant of the invisble aluminum spins in zeolite HY with 1H/27Al. *Journal of the American Chemical Society*, **117**, 8232–8242.

Gullion T. (1995) Measurement of dipolar interactions between spin-1/2 and quadrupolar nuclei by rotational-echo, adiabatic-passage, double-resonance NMR. *Chemical Physics Letters*, **246**, 325–330.

Gullion T. & Schaefer J. (1989) Detection of weak heteronuclear dipolar coupling by rotational-echo double-resonance nuclear magnetic resonance. *Advances in Magnetic Resonance*, Vol. **13**. Academic Press, San Diego, pp. 57–83.

Hanaya M. & Harris R.K. (1997) Effect of ^{1}H-decoupling in two-dimensional multiple-quantum MAS NMR spectroscopy of ^{23}Na in a hydrous layered silicate. *Solid State Nuclear Magnetic Resonance*, **8**, 147–151.

Hanaya M. & Harris R.K. (1998) Two-dimensional ^{23}Na MQMAS NMR study of layered materials. *Journal of Materials Chemistry*, **8**, 1073–1079.

Hayashi S. (1997) Solid-state NMR study of locations and dynamics of interlayer cations and water in kanemite. *Journal of Materials Chemistry*, **7**, 1043–1048.

Kanehashi K. & Saito K. (2002) Investigation on chemical structure of inorganic matter in coal by ^{27}Al MQMAS and ^{1}H→^{27}Al CP/MQMAS NMR. *Journal of the Iron and Steel Institute of Japan*, **88**, 730–735.

Kentgens A.P.M. & Verhagen R. (1999) Advantages of double frequency sweeps in static, MAS and MQMAS NMR of spin I=3/2 nuclei. *Chemical Physics Letters*, **300**, 435–443.

Lee S.K. & Stebbins J.F. (2003) O atom sites in natural kaolinite and muscovite: O-17 MAS and 3QMAS NMR study. *American Mineralogist*, **88**, 493–500.

Lee S.K., Stebbins J.F., Weiss C.A. & Kirkpatrick R.J. (2003) ^{17}O and ^{27}Al MAS and 3QMAS NMR study of synthetic and natural layer silicates. *Chemistry of Materials*, **15**, 2605–2613.

Levitt M.H. (2001) *Spin Dynamics, Basics of Nuclear Magnetic Resonance*. John Wiley & Sons, Ltd, Chichester, UK.

Lim K.H. & Grey C.P. (1998) Analysis of the anisotropic dimension in the RIACT (II) MQMAS NMR experiment for I=3/2 nuclei. *Solid State Nuclear Magnetic Resonance*, **13**, 101–112.

Lim K.H. & Grey C.P. (1999) Triple-quantum cross-polarization NMR of ^{1}H/^{27}Al and ^{19}F/^{23}Na spin systems in solids. *Chemical Physics Letters*, **312**, 45–56.

Llor A. & Virlet J. (1988) Towards high-resolution technique NMR of more nuclei in solids: sample spinning with time-dependent spinner axis angle. *Chemical Physics Letters*, **152**, 248–253.

Madhu P.K & Levitt M.H. (2002) Signal enhancement in the triple-quantum Magic-Angle-Spinning NMR of spin-3/2 in solids: The FAM-RIACT-FAM sequence. *Journal of Magnetic Resonance*, **155**, 150–155.

Madhu P.K., Goldbourt A., Frydman L. & Vega S. (1999) Sensitivity enhancement of the MQMAS NMR experiment by fast amplitude modulation of the pulses. *Chemical Physics Letters*, **307**, 41–47.

Madhu P.K., Goldbourt A., Frydman L. & Vega S. (2000) Fast radio-frequency amplitude modulation in multiple-quantum magic-angle-spinning nuclear magnetic resonance: Theory and experiments. *Journal of Chemical Physics*, **112**, 2377–2391.

Man P.P., Klinowski J., Trokiner A., Zanni H. & Papon P. (1988) Selective and non-selective NMR excitation of quadrupolar nuclei in the solid state. *Chemical Physics Letters*, **151**, 143–150.

Marinelli L., Medek A. & Frydman L. (1998) Composite pulse excitation schemes for MQMAS NMR of half-integer quadrupolar spins. *Journal of Magnetic Resonance*, **132**, 88–95.

Massiot D. (1996) Sensitivity and lineshape improvements of MQ-MAS by rotor synchronized data acquisition. *Journal of Magnetic Resonance A*, **122**, 240–244.

Massiot D., Touzo B., Trumeau D., Coutures J.P., Virlet J., Florian P. & Grandinetti P.J. (1996) Two-dimensional magic-angle-spinning isotropic reconstruction sequences for quadrupolar nuclei. *Solid State Nuclear Magnetic Resonance*, **6**, 73–83.

Massiot D., Montouillout V., Fayon F., Florian P. & Bessada C. (1997) Order-resolved sideband separation in magic-angle-spinning NMR of half-integer quadrupolar nuclei. *Chemical Physics Letters*, **272**, 295–300.

Massiot D., Vosegaard T., Magneron N., Trumeau D., Montouillout V., Berthet P., Loiseau T. & Bujoli B. (1999) ^{71}Ga NMR of reference Ga^{IV}, Ga^{V} and Ga^{VI} compounds by MAS and QPASS, extension of gallium/aluminium NMR parameters correlation. *Chemical Physics Letters*, **272**, 295–300.

Massiot D., Fayon F., Capron M., King I., Le Calvé S., Alonso B., Durand J.O., Bujoli B., Gan Z. & Hoatson G. (2002) Modelling one and two-dimensional solid-state NMR spectra. *Magnetic Resonance in*

Chemistry, **40**, 70–76.

Morais C.M., Lopes M., Fernandez C. & Rocha J. (2003) Assessing the potential of fast amplitude modulation pulses for improving triple-quantum magic angle spinning NMR spectra of half-integer quadrupolar nuclei. *Magnetic Resonance in Chemistry* (in press).

Pruski M., Lang D.P., Fernandez C. & Amoureux J.P. (1997) Multiple-quantum magic-angle-spinning NMR with cross-polarization: Spectral editing of high-resolution spectra of quadrupolar nuclei. *Solid State Nuclear Magnetic Resonance*, **7**, 327–331.

Pruski M., Baily A., Lang D.P., Fernandez C. & Amoureux J.P. (1999) Studies of heteronuclear dipolar interactions between spin-1/2 and quadrupolar nuclei by using REDOR during multiple-quantum evolution. *Chemical Physics Letters*, **307**, 35–40.

Rocha J. (1999) Single and triple quantum ^{27}Al MAS NMR study of the thermal transformation of kaolinite. *Journal of Physical Chemistry B*, **103**, 9801–9804.

Rocha J., del Arco M., Rives V. & Ulibarri A. (1999) Reconstruction of layered double hydroxides from calcined percursors: a powder XRD and ^{27}Al MAS NMR study. *Journal of Materials Chemistry*, **9**, 2499–2503.

Rovnyak D., Baldus M. & Griffin R.G. (2000) Multiple-quantum cross polarization in quadrupolar spin systems during Magic-Angle Spinning. *Journal of Magnetic Resonance*, **142**, 145–152.

Samoson A. & Lippmaa E. (1983) Central transition NMR excitation spectra of half-integer quadrupole nuclei. *Chemical Physics Letters*, **100**, 205–208.

Samoson A., Lipmaa E. & Pines A. (1988) High resolution solid state NMR averaging of second-order effects by means of a double-rotor. *Molecular Physics*, **65**, 1013–1018.

Schäfer H., Iuga D., Verhagen R. & Kentgens A.P.M. (2000) Population and coherence transfer in half-integer quadrupolar spin systems induced by simultaneous rapid passages of the satellite transitions: A static and spinning single crystal NMR study. *Journal of Chemical Physics*, **114**, 3073–3091.

Smith S.A., Levante T.O., Meier B.H. & Ernst R.R. (1994) Computer simulations in magnetic resonance. An object-oriented programming approach. *Journal of Magnetic Resonance A*, **106**, 75–105.

Stebbins J.F., Du L.S., Kroeker S., Neuhoff P., Rice D., Frye J. & Jakobsen H.J. (2002) New opportunities for high-resolution solid-state NMR spectroscopy of oxide materials at 21.1- and 18.8-T fields. *Solid State Nuclear Magnetic Resonance*, **21**, 105–115.

Tuel A., Gramlich V. & Baerlocher Ch. (2001) Synthesis, crystal structure and characterization of AP2DAO, a new layered aluminophosphate templated by 1,8-diaminooctane molecules. *Microporous and Mesoporous Materials*, **47**, 217–229.

Tuel A., Gramlich V. & Baerlocher Ch. (2001) Synthesis, structure determination and characterization of a new layered aluminophosphate templated by piperazinium ions. *Microporous and Mesoporous Materials*, **46**, 57–66.

Tuel A., Gramlich V. & Baerlocher Ch. (2002) Synthesis, characterization and structure determination of two novel layered aluminophosphates templated by 2-methylpiperazine. *Microporous and Mesoporous Materials*, **56**, 119–130.

Van Eck E.R.H., Janssen R., Maas W.E.J.R. & Veeman W.S. (1990) A novel application of nuclear spin-echo double-resonance to aluminophosphates and aluminosilicates. *Chemical Physics Letters*, **174**, 428–432.

Vega A.J. (1992) MAS NMR spin locking of half-integer quadrupolar nuclei. *Journal of Magnetic Resonance*, **96**, 50–68.

Vega S. & Naor Y. (1981) Triple-quantum NMR on spin systems with I=3/2 in solids. *Journal of Chemical Physics*, **75**, 75–86.

Vosegaard T., Larsen F.H., Jakobsen H.J., Ellis P.D. & Nielsen C.N. (1997) Sensitivity-enhanced multiple-quantum MAS NMR of half-integer quadrupolar nuclei. *Journal of the American Chemical Society*, **122**, 9055–9056.

Vosegaard T., Massiot D. & Grandinetti P.J. (2000) Sensitivity enhancements in MQ-MAS NMR of spin-5/2 nuclei using modulated *rf* mixing pulses. *Chemical Physics Letters*, **326**, 454–460.

Vosegaard T., Florian P., Massiot D. & Grandinetti P.J. (2001) Multiple quantum magic-angle spinning using rotary resonance excitation. *Journal of Chemical Physics*, **114**, 4618–4624.

Wang P.K., Slichter C.P. & Sinfelt J.H. (1984) NMR study of the structure of simple molecules adsorbed on metal surfaces: C_2H_2 on Pt, *Physical Review Letters*, **53**, 82–85

Wang S.H., De Paul S.M. & Bull L.M. (1997) High-resolution heteronuclear correlation between quadrupolar and spin 1/2 nuclei using multiple-quantum magic-angle spinning. *Journal of Magnetic Resonance*, **125**, 364–368.

Wu G., Rovnyak D. & Griffin R.G. (1996) Quantitative MQMAS NMR spectroscopy of quadrupolar nuclei in solids. *Journal of the American Chemical Society*, **118**, 9326–9332.

Yao Z., Kwak H.T., Sakellariou D., Emsley L. & Grandinetti P.J. (2000) Sensitivity enhancement of the central transition NMR signal of quadrupolar nuclei under magic angle spinning. *Chemical Physics Letters*, **327**, 85–90.